

The Impact of Assimilating SSM/I and QuikSCAT Satellite Winds on Hurricane Isidore Simulations

SHU-HUA CHEN

Department of Land, Air, and Water Resources, University of California, Davis, Davis, California

(Manuscript received 7 December 2005, in final form 6 April 2006)

ABSTRACT

Three observational datasets of Hurricane Isidore (in 2002) were analyzed and compared: the Special Sensor Microwave Imager (SSM/I), the Quick Scatterometer (QuikSCAT) winds, and dropsonde winds. SSM/I and QuikSCAT winds were on average about 1.9 and 0.3 m s⁻¹ stronger, respectively, than dropsonde winds. With more than 20 000 points of data, SSM/I wind speed was about 2.2 m s⁻¹ stronger than QuikSCAT. Comparison of the wind direction observed by QuikSCAT with those from the dropsondes showed that the quality of QuikSCAT data is good. The effect of assimilating SSM/I wind speeds and/or QuikSCAT wind vectors for the analysis of Hurricane Isidore was assessed using the fifth-generation Pennsylvania State University–National Center for Atmospheric Research (PSU–NCAR) Mesoscale Model (MM5) and its three-dimensional variational data assimilation system. For the Hurricane Isidore case study, it was found that the assimilation of either satellite winds strengthened the cyclonic circulation in the analysis. However, the increment of the QuikSCAT wind analysis is more complicated than that from the SSM/I analysis due to the correction of the storm location, a positive result from the assimilation of wind vectors. The increase in low-level wind speeds enhanced the air–sea interaction processes and improved the simulated intensity for Isidore. In addition, the storm structure was better simulated. Assimilation of QuikSCAT wind vectors clearly improved simulation of the storm track, in particular during the later period of the simulation, but lack of information about the wind direction from SSM/I data prevented it from having much of an effect. Assessing the assimilation of QuikSCAT wind speed versus wind vector data confirmed this hypothesis. The track improvement partially resulted from the relocation of the storm's initial position after assimilation of the wind vectors. For this case study, it was found that the assimilation of SSM/I or QuikSCAT data had the greatest impact on the Hurricane Isidore simulation during the first 2 days.

1. Introduction

The initial condition is one of the key components to accurate numerical weather simulations and forecasts. Data sparseness used to be one of the primary concerns for numerical weather forecasts and climate studies in oceanic, tropical, and polar regions. In the last two decades, however, data sparseness has been less of a problem as advanced satellite technologies and instruments have contributed a great amount of data to the existing observational networks. Compared with conventional upper-air radiosondes, the high spatial and temporal

resolutions of satellites (the latter generally applies only to geostationary satellites) make them particularly attractive. However, sun-synchronous polar-orbiting satellites pass the same region on the earth only twice daily. As a result, satellite observations might not be available in a target region at the initial time. Therefore, the synthesis of different sources of data has become one of the most important issues to data assimilation, particularly for operational centers where forecasts are performed on a daily basis.

Due to the coupling of near-surface winds to boundary layer processes (e.g., heat and momentum exchanges between the atmosphere and ocean), they, along with moisture and temperature, play an important role in severe marine weather development. Fortunately, several satellites have observed winds over the ocean during the last two decades, such as the *Geo-*

Corresponding author address: Dr. Shu-Hua Chen, Department of Land, Air, and Water Resources, University of California, Davis, One Shields Ave., Davis, CA 95616-8627.
E-mail: shachen@ucdavis.edu

sat altimeter, the National Aeronautics and Space Administration (NASA) Scatterometer (NSCAT), the Quick Scatterometer (QuikSCAT), the Special Sensor Microwave Imager (SSM/I), European Space Agency Remote Sensing Satellites (*ERS-1/2*), and water vapor or cloud-derived satellite winds. Comparisons between different observed surface winds or between observed winds and model forecasted/analyzed winds have been studied extensively (Halpern et al. 1994; Rienecker et al. 1996; Boutin and Etcheto 1996; Meissner et al. 2001; Mears et al. 2001; Yuan 2004), but no comparisons have been made between SSM/I and QuikSCAT. Boutin and Etcheto (1996) found that SSM/I-retrieved wind speeds are underestimated by more than 1 m s^{-1} with respect to ship measurements at high latitudes. However, when compared with *ERS-1*, SSM/I winds are overestimated by $0.5\text{--}1 \text{ m s}^{-1}$ over regions where the atmospheric water content is high. It has also been found that SSM/I winds derived from Wentz's algorithm (Wentz 1993) are systematically overestimated in regions of higher water vapor content (Halpern 1993; Waliser and Gautier 1993; Boutin and Etcheto 1996). A neural network algorithm, which takes into account the nonlinear relationship between wind speeds and brightness temperatures, has also been used to derive the SSM/I winds and has produced promising results (Stogryn et al. 1994; Krasnopolsky et al. 1995; Yu et al. 1997).

Most studies of satellite-observed low-level winds have concentrated on data comparisons. Few focus on the use of data assimilation techniques to improve analysis and model simulations (Phalippou 1996; Yu et al. 1997; Zou and Xiao 2000; Isaksen and Stoffelen 2000; Atlas et al. 2001; Leidner et al. 2003; Chen et al. 2004; Isaksen and Janssen 2004). Isaksen and Stoffelen (2000) showed a positive impact of assimilating ERS scatterometer wind data on tropical cyclone analysis and forecasts using a four-dimensional variational data assimilation technique (4DVAR). The *ERS-1/2* C-band instrument measures winds that are not contaminated by heavy precipitation. However, the width of the swath (500 km) is quite narrow. In similar studies, Leidner et al. (2003) assimilated NSCAT using 4DVAR to improve tropical cyclone forecasts, and Isaksen and Janssen (2004) assimilated ERS winds using 4DVAR and 3DVAR (i.e., four- and three-dimensional variational data assimilation techniques, respectively) to improve analysis and tropical cyclone and polar-low forecasts. These studies showed that the variational data assimilation method allows consistent propagation of surface wind information throughout the troposphere. Chen et al. (2004) used 3DVAR to assess the impact of assimilating retrieved SSM/I products (e.g., winds and total column water vapor) for Hur-

ricane Danny (in 1997) simulations. Their results showed very promising improvement for simulated storm intensity, but little improvement for the simulated storm track. The improvement of the simulated track has been studied using different techniques such as a variational bogus data assimilation scheme (Zou and Xiao 2000) and a vortex specification scheme (Kurihara et al. 1993; Bender et al. 1993).

In this study, our purpose is to analyze the characteristics of SSM/I and QuikSCAT winds and to investigate their impact on Hurricane Isidore (in 2002) simulations. It is well known that QuikSCAT winds consist of both wind speed and direction, while for SSM/I only wind speed is available. Therefore, we also investigate the importance of assimilating satellite-observed wind direction on model simulations. This type of study can help us make better use of different observations and design new observation networks in the future. However, results presented here are based on one case study only, and more studies are required in order to draw general conclusions. The fifth-generation Pennsylvania State University–National Center for Atmospheric Research (PSU–NCAR) Mesoscale Model (MM5; Grell et al. 1994) and its three-dimensional data assimilation system (Barker et al. 2004) are utilized.

This paper is organized as follows: section 2 introduces the variational assimilation system and assimilated data. The storm description, model configuration, and experimental design are presented in section 3. Results are discussed in section 4, and a brief summary is given in section 5.

2. Variational assimilation system and assimilated data

a. The 3DVAR system

The MM5 3DVAR (Barker et al. 2004) uses the multivariate incremental formulation (Courtier et al. 1994). Following Lorenc et al. (2000), the control variables are the streamfunction, velocity potential, unbalanced pressure, and relative humidity. Error correlations between control variables are neglected except for a constraint on mass and winds, whereby geostrophic or cyclostrophic balance can be enforced. A statistical regression is used to ensure that the balanced pressure is used only where appropriate (Barker et al. 2004). The National Meteorological Center (NMC) method (Parish and Derber 1992) is applied to generate the background error covariances using the MM5 real-time daily forecasts at NCAR on a 30-km grid over the continental United States. An example of the horizontal and vertical structure functions generated from the

method and used in this study can be found in Chen et al. (2004).

The MM5 3DVAR system used here can assimilate conventional data and some nonconventional data, such as SSM/I and QuikSCAT satellite measurements. The observation errors are assumed to be uncorrelated, therefore resulting in a diagonal observational error covariance matrix. The cost function includes a background and an observational term. In this study, the observational term of the cost function is contributed from SSM/I and QuikSCAT data only since no other observations are assimilated. A detailed description of the MM5 3DVAR system is given in Barker et al. (2004).

b. SSM/I data

The SSM/I is a conical scanning, four-frequency, linearly polarized, seven-channel passive microwave radiometer. The first SSM/I instrument was launched aboard the Defense Meteorological Satellite Program (DMSP) of the U.S. Navy in June 1987. This polar-orbiting satellite has a period of about 102 min. The instrument has a near-constant incidence angle of 53° , a mean altitude of approximately 830 km, and a swath width of about 1400 km. SSM/I data are available under both clear and cloudy oceanic conditions but can be contaminated by heavy precipitation. Detailed information about the SSM/I instrument may be found in Hollinger (1989).

The retrieved total column water vapor and sea surface winds from DMSP *F13* and *F14* satellites were used in this study. The data resolution is 25 km, comparable to that of the larger domain (i.e., domain 1) in the model configuration (30 km). The total column water vapor and the sea surface wind were both derived from brightness temperatures using Wentz's algorithm (1993). Following Chen et al. (2004), the observational error variances (σ_o^2) for SSM/I sea surface wind speed and total column water vapor are $2.5^2 \text{ m}^2 \text{ s}^{-2}$ and 2^2 mm^2 , respectively.

c. QuikSCAT data

The QuikSCAT satellite was launched in 1999. The SeaWinds instrument aboard the QuikSCAT satellite is a 13.4-GHz Ku-band conical-scanning microwave radar that measures backscattered power. The observations from SeaWinds replace data formerly obtained from the NSCAT, which lost power in 1997. This polar-orbiting satellite has a period of about 101 min. The QuikSCAT satellite's maximum altitude is approximately 800 km, and its swath width is about 1800 km. Like SSM/I data, QuikSCAT winds can be measured

under both clear and cloudy conditions over oceans and the data are also contaminated by heavy precipitation.

QuikSCAT level-2B wind vectors derived from the Wentz and Smith's model (1999) are used in this study. The resolution of QuikSCAT winds is 25 km, which is the same as that of SSM/I data. In addition to the wind speed, QuikSCAT can also collect information on wind direction, a feature lacking in SSM/I. This additional information obtained by QuikSCAT has the potential to make an extra contribution to 3DVAR analysis. The observational error variance (σ_o^2) for the u and v components of QuikSCAT wind vectors is $1.4^2 \text{ m}^2 \text{ s}^{-2}$, which is the default value in the MM5 3DVAR system.

d. Data quality control

Scatterometer wind measurements (e.g., QuikSCAT, NSCAT, and *ERS-1/2*) suffer from ambiguities. QuikSCAT data can include up to four possible wind vectors. The ambiguities can be removed as part of the variational assimilation process by introducing a non-quadratic cost function for scatterometer data (Leidner et al. 2003; Isaksen and Janssen 2004). In this study, the direction interval retrieval, which enhances the modified median-filter-based algorithm (Shaffer et al. 1991), with threshold nudging wind vector solution was applied to select the best wind vector among these ambiguities. The removal of the ambiguities was performed before QuikSCAT data were presented to the MM5 3DVAR system.

Prior to data assimilation, both SSM/I and QuikSCAT data underwent several quality checking processes in order to reduce the possibility of assimilating bad observations. First, data collected over land and ice were excluded. Second, the quality of retrieved high winds is questionable due to the saturation of signals. Therefore, observations with wind speeds greater than 30 m s^{-1} were removed for both satellites. Third, since the polar-orbiting satellite receives data signals continuously, a time window for data cutoff was applied. We chose a 3-h time window (1.5 h before and after the initial time) as the storm was moving slowly around the model initial time. This window is not too long but enough so that sufficient data will be included. Finally, a gross error quality control was performed. Observations that differed from the model's background (i.e., first guess) by more than 5 times the observation error were removed. The number 5 is a default value in the MM5 3DVAR system. However, with this default value, too many QuikSCAT wind vectors were removed due to the mismatch of storm locations between the background and the best-track position. Some of the removed wind vectors may be important for improving the storm intensity and location if it is mis-

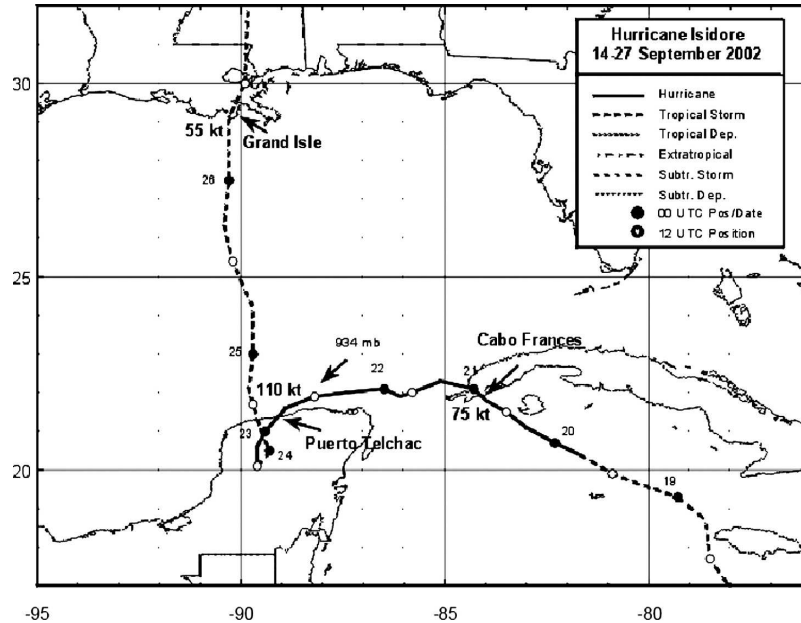


FIG. 1. Best-track positions for Hurricane Isidore from 18 to 26 Sep 2002 (courtesy of the NOAA/National Hurricane Center).

placed in the background field. Therefore, in this study a value of 6 instead of 5 was used for QuikSCAT wind gross error quality control so that some wind vectors over the storm region were kept for assimilation, while some of them were removed. One should be cautious in employing the gross error check because it can potentially eliminate good quality data. This problem can be reduced if an outer iteration technique is applied (Li et al. 2000; Rabier et al. 2000). The outer iteration allows the update of the background states during the assimilation process; however, this is not implemented in this earlier version of the MM5 3DVAR code.

3. Experimental design

a. Hurricane Isidore

Although many oceanic observations are available, it is generally difficult to find two or more independent datasets from the same time and location when investigating specific events like a hurricane. Hurricane Isidore was chosen for this study because observations from SSM/I, QuikSCAT, and the global positioning system (GPS) dropsondes, collected by the National Oceanic and Atmospheric Administration (NOAA) reconnaissance planes, were all available over the storm region at the model initial time.

Figure 1 shows the best-track positions of Hurricane Isidore. Isidore started as a tropical wave off the coast of Africa on 9 September 2002. It became a tropical

storm around 0600 UTC 18 September just west of Jamaica and a weak steering flow resulted in its slow movement northwest. The storm was classified as a hurricane at 1800 UTC 19 September 2002. Isidore reached a maximum intensity of 55 m s^{-1} at 1800 UTC 21 September 2002; however, the pressure at the storm center continued to deepen, reaching a minimum of 934 mb at 1200 UTC 22 September 2002 near the north coast of the Yucatan. The storm moved anomalously southwest over the Yucatan, a movement that the National Hurricane Center official forecast failed to capture. After 0000 UTC 24 September 2002, Isidore moved in a northward direction over the Gulf of Mexico, making landfall in Louisiana at 0600 UTC 26 September 2002. The average track errors in the official forecasts for Hurricane Isidore were about 59, 102, 135, 187, and 328 km for the 12-, 24-, 36-, 48-, and 72-h forecasts, respectively. These errors are smaller than 10-yr average errors. The average errors of maximum low-level winds were about 4.5, 8, 11, 15, and 23 m s^{-1} for the 12-, 24-, 36-, 48-, and 72-h forecasts, respectively. [More information about Isidore can be found in the National Centers for Environmental Prediction (NCEP) preliminary report online at www.nhc.noaa.gov/2002isidore.shtml.]

b. Experiments

The MM5 model was used for all numerical simulations in this study. Figure 2 shows the two domains superimposed with the terrain of domain 1. The reso-

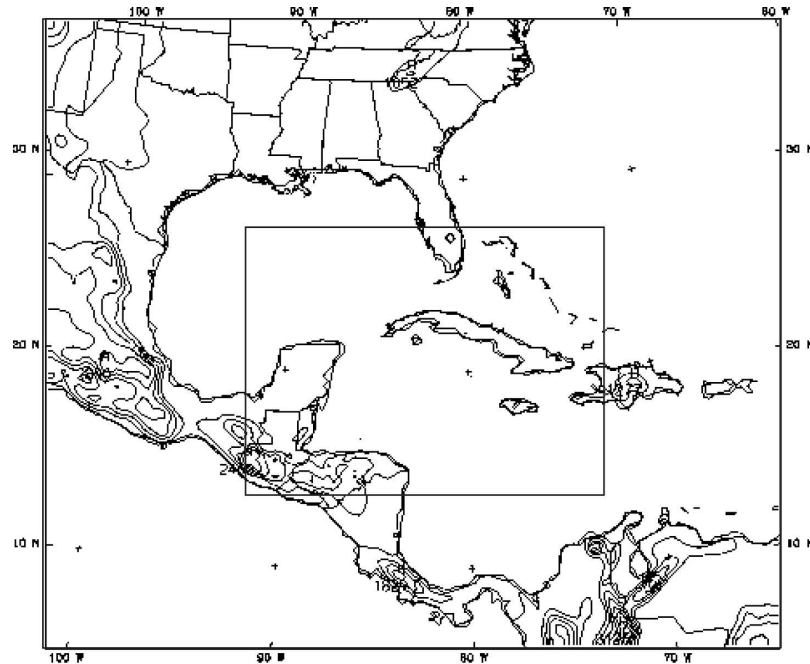


FIG. 2. Two nested domains used in MM5 model simulations. The resolutions are 30 and 10 km for domains 1 (larger one) and 2 (smaller one), respectively. The contours are terrain elevation on domain 1 with a contour interval of 500 m.

lutions for domains 1 (larger one) and 2 (smaller one) are 30 and 10 km, respectively. The grid's dimensions are $140 \times 120 \times 31$ and $208 \times 151 \times 31$ in east–west, north–south, and vertical directions in domains 1 and 2, respectively. The model extends from the surface up to 100 hPa.

Seven numerical experiments (Table 1) with various initial conditions were conducted using two-domain (Fig. 2), two-way interaction simulations. Data from the NCEP–NCAR reanalysis project (NNRP; Kalnay et al. 1996) with a $2.5^\circ \times 2.5^\circ$ resolution were used to provide boundary conditions. Instead of directly using NNRP data for the first guess in the 3DVAR experiments, an MM5 simulation using one domain only (i.e., domain 1 in Fig. 2) was first integrated from 1800 UTC 18 September 2002 for 6 h to provide a 3DVAR first guess at 0000 UTC 19 September 2002. The CNTL experiment continued the 6-h simulation but used two domains after 0000 UTC 19 September 2002. Figure 3 shows the horizontal cross sections of the synoptic-scale fields of the NNRP reanalysis at 1800 UTC 18 September 2002. The storm center, which is defined by the 950-hPa circulation center (or minimum wind speed), was about 150 km southwest of the best-track position (Fig. 3a). After a 6-h simulation (i.e., at 0000 UTC 19 September 2002), the storm was about 250 km west of the best-track position (see black dots in Fig. 4), which is used for comparison in this study. This discrepancy provides

a great opportunity to assess the impact of wind observations on hurricane analyses and simulations.

For the numerical simulations presented in Table 1, satellite winds were assimilated for domain 1 only. The initial conditions of domain 2 were interpolated from 3DVAR analyses of domain 1. The new Kain–Fritsch cumulus parameterization (Kain 2004), which includes deep and shallow convection, medium-range frequency (MRF) boundary layer parameterization (Hong and Pan 1996), mixed-phase microphysics, and a cloud radiation scheme were activated. For each simulation, the model integrated 72 h starting from 0000 UTC 19 September 2002. The time step for domain 1 is 90 s.

The MM5 3DVAR system was used to assimilate observations, including QuikSCAT winds and SSM/I-

TABLE 1. Assimilated data for each numerical experiment.

Case	Assimilated data
CNTL	None
SSW	SSM/I sea surface wind speeds
TSSW	Same as SSW plus SSM/I total column water vapor
QCAT	QuikSCAT wind speeds and directions
TQCAT	Same as QCAT plus SSM/I total column water vapor
NDQCAT	QuikSCAT wind speeds
ALL	SSM/I total column water vapor SSM/I sea surface wind speeds QuikSCAT wind speeds and directions

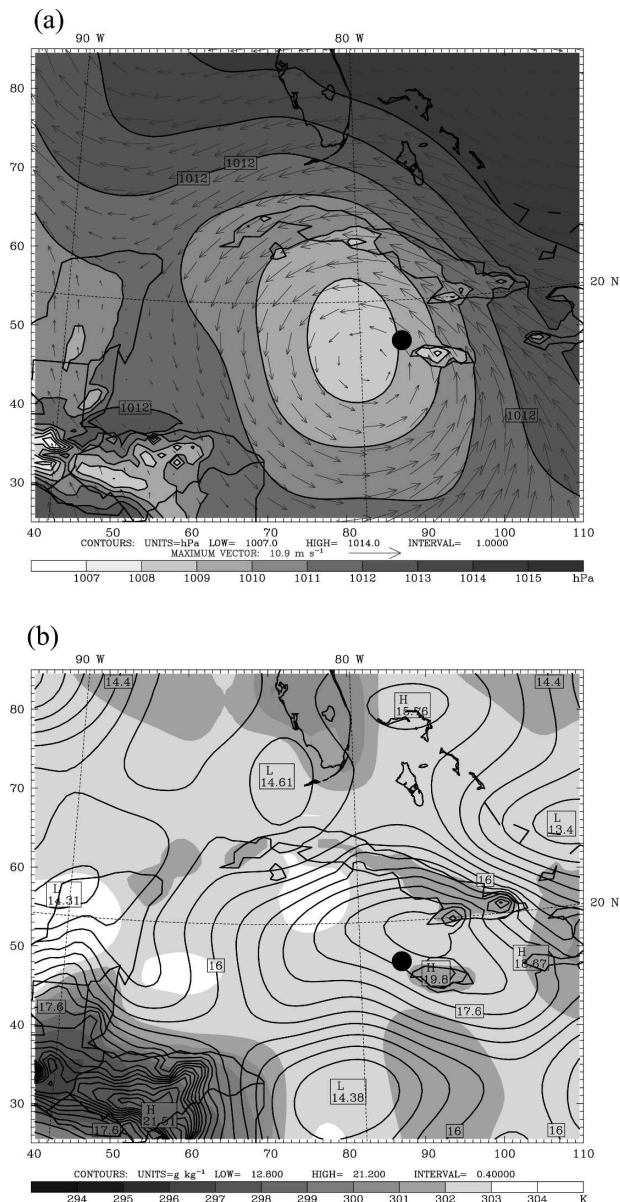


FIG. 3. The horizontal cross sections of the (a) sea level pressure (SLP; hPa; shaded with contours) and 950-hPa wind vectors, and (b) 500-m water vapor mixing ratio (g kg^{-1} ; contours) and temperature (shaded; K) at 1800 UTC 18 Sep 2002 for part of domain 1. The black dot indicates the best-track position of the storm center. The contour intervals for the SLP and water vapor mixing ratio are 1 hPa and 0.4 g kg^{-1} , respectively.

retrieved total column water vapor and sea surface winds. The experiments in Table 1 overestimate the impact of the SSM/I and QuikSCAT data because other observations (e.g., dropsondes) have been left out. Figure 4 shows the SSM/I and QuikSCAT data coverage area within a 3-h time window centered at the model initial time. Fortunately, both observations have one

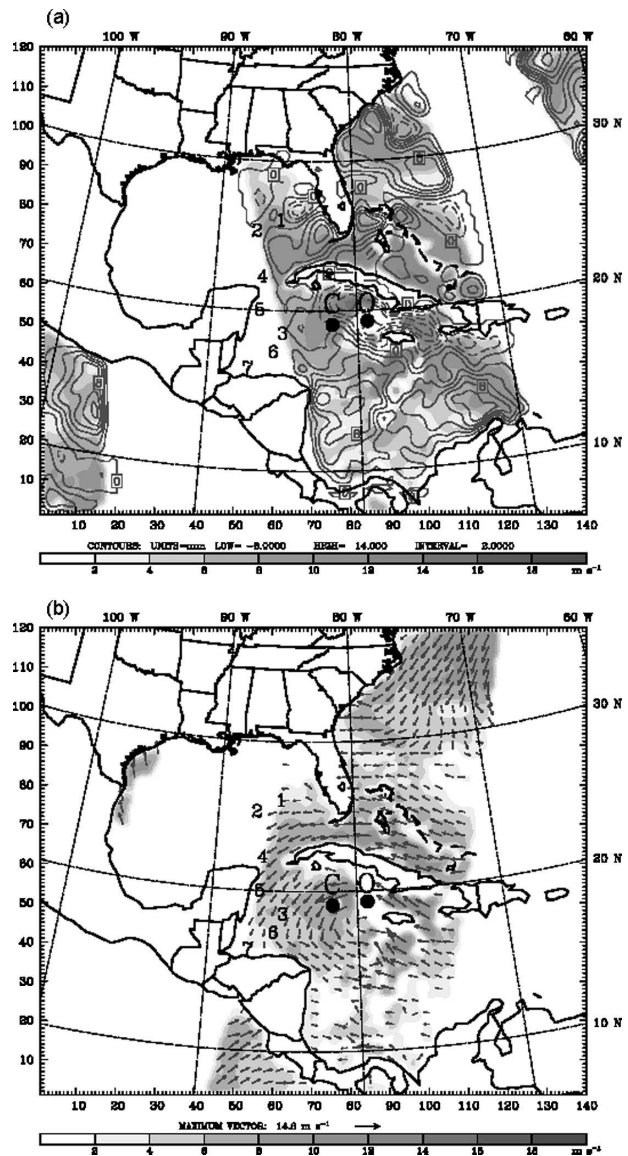


FIG. 4. The coverage area of the (a) SSM/I and (b) QuikSCAT data used within a 3-h time window (2230 UTC 18 Sep–0130 UTC 19 Sep 2002). (a) SSM/I-retrieved sea surface wind speeds (shaded; m s^{-1}) and the innovation of SSM/I total column water vapor (i.e., observation minus first guess; gray contour lines; mm), while (b) QuikSCAT wind speeds (shaded; m s^{-1}) and wind vectors. East (west) black dot with the letter O (C) indicates Hurricane Isidore's best-track position (CNTL experiment) at 0000 UTC 19 Sep 2002. Numbers indicate seven GPS-dropsonde locations. The swath passing through the storm is 36 (73) min earlier (later) than the model initial time (0000 UTC 19 Sep 2002) for QuikSCAT (SSM/I) data.

swath of data over the best-track position of the storm center (represented as a black dot with an O). The observational time for the main swath of QuikSCAT data passing over the storm is about 36 min earlier than the model initial time (i.e., 0000 UTC 19 Septem-

TABLE 2. Winds from GPS dropsondes, SSM/I, and QuikSCAT at 10-m height. The wind speeds (m s^{-1}) from dropsondes are interpolated to 10-m height, while its wind directions ($^{\circ}$) are taken from the lowest available observed level. The distance (km) and time difference (min) between dropsonde and SSM/I (QuikSCAT) are provided in the parentheses.

Point	Dropsonde wind speed	SSM/I wind speed	QuikSCAT wind speed	Dropsonde wind direction	QuikSCAT wind direction
1	4.39	7.64 (11 km, 116 min)	3.85 (28 km, 4 min)	47.5	74.0
2	7.42	8.10 (68 km, 5 min)	5.60 (181 km, 117 min)	92.6	62.8
3	5.31	7.01 (66 km, 123 min)	5.57 (14 km, 15 min)	29.3	25.3
4	5.93	9.01 (107 km, 88 min)	7.03 (67 km, 22 min)	63.8	52.3
5	5.65	6.77 (183 km, 106 min)	5.80 (34 km, 3 min)	47.1	40.2
6	3.23	5.77 (210 km, 136 min)	3.88 (10 km, 28 min)	327.3	5.0
7	4.04	8.33 (359 km, 148 min)	4.02 (51 km, 41 min)	17.1	27.0

ber 2002), while that of SSM/I data is about 73 min later.

The standard experiment, CNTL, was used for comparison purposes since it did not assimilate any observational data. SSW and QCAT, which assimilated SSM/I and QuikSCAT winds, respectively, were conducted to assess the impact of the two types of satellite-observed winds on hurricane simulations. TSSW and TQCAT are similar to SSW and QCAT, respectively, but with the additional assimilation of SSM/I-retrieved total column water vapor. The impact of assimilating SSM/I-retrieved moisture alone on the Isidore simulation is negative. Since our primary interest is satellite winds, the experiment with the assimilation of this moisture data only has been examined but is not included in the table. Generally, the locations of storms and fronts were not predicted well. Information from observed wind vectors (e.g., QuikSCAT winds) can be assimilated to potentially correct the locations of those systems, thus affecting position simulations/forecasts. Therefore, NDQCAT, which assimilated only QuikSCAT wind speeds, was designed to examine the influence of wind directions on Isidore simulation. Observations from SSM/I and QuikSCAT are independent and the assimilation of all data (i.e., ALL) was also assessed.

4. Results and discussion

a. Observations

From SSM/I and QuikSCAT swath data (Fig. 4), the storm is clearly surrounded by high winds whose strength is greater than the first guess (i.e., 6-h simulation with MM5 from NCEP–NCAR reanalysis; figure not shown). Yet a cyclonic circulation is also observed from QuikSCAT wind vectors (Fig. 4b) and it is approximately east-southeast of the one in the first guess (represented by a black dot C). Therefore, the assimilation of wind observations is expected to enhance initial circulation of the storm. Additionally, the assimila-

tion of wind vector observations is more likely to move the tropical storm location than just using wind speed. It is noticed that the location of the Isidore center determined from QuikSCAT winds is not in agreement with the best track. Moreover, some of the QuikSCAT ambiguities southeast of the best-track storm location (Fig. 4b) are incorrect, but those data were filtered out by the gross error quality check before the assimilation. Data from both satellites close to the best-track position of the storm center (black dot O) are missing because of contamination from heavy precipitation and, in consequence, the exact storm center from the QuikSCAT wind vectors cannot be clearly defined.

The innovation (i.e., observation minus first guess) of SSM/I-retrieved total column water vapor is plotted in Fig. 4a (contours). Although a large portion of the SSM/I middle swath has positive innovations, there is a negative zone (dashed contours) that passes through the storm location. This negative zone is oriented in the northwest–southeast direction, nearly parallel to Cuba.

Fortunately, a special hurricane field experiment was conducted by NOAA and NCAR for Hurricane Isidore. Therefore, another independent dataset, GPS dropsondes, is available for our case study. Within a 3-h time window (i.e., from 2230 UTC 18 September to 0130 UTC 19 September 2002), seven GPS dropsondes were found to overlap with SSM/I and/or QuikSCAT data (numbers 1–7 in Fig. 4); however, they were far away from the center of Isidore and the wind speeds were weak, about 3–7 m s^{-1} . Attention should also be paid to the fact that several GPS dropsondes were located near the edge of the SSM/I or QuikSCAT swaths.

Table 2 shows the 10-m winds from GPS dropsonde, SSM/I, and QuikSCAT observations. The distance and time differences between dropsonde and SSM/I or QuikSCAT are provided in the parentheses. Here, we assume that data from GPS dropsondes are reliable and thus can be used for comparisons with the other two observations (i.e., SSM/I and QuikSCAT). For those

points whose distances from dropsondes are less than 100 km (Table 2), the average wind discrepancy (or error) was about 1.9 m s^{-1} for SSM/I winds (points 1, 2, and 3) and 0.3 m s^{-1} for QuikSCAT winds (points 1, 3, 4, 5, 6, and 7). Their corresponding standard deviations were 2.2 and 0.6 m s^{-1} for SSM/I and QuikSCAT, respectively. Although few GPS dropsonde soundings are available, the result indicates that the quality of QuikSCAT winds data is slightly better than SSM/I data, a result that is qualitatively consistent with the error variances mentioned in section 2 ($2.5^2 \text{ m}^2 \text{ s}^{-2}$ for SSM/I and $1.4^2 \text{ m}^2 \text{ s}^{-2}$ for QuikSCAT). Compared with dropsondes, the QuikSCAT wind direction within the same distance (i.e., 100 km) had an average discrepancy of about 8.6° and the standard deviation was about 20° .

Figure 5 shows the point density plot of the SSM/I versus QuikSCAT wind speeds (21 247 data points). Data were collected from 1200 UTC 17 September to 1200 UTC 23 September 2002 within domain 1. The maximum spatial and temporal separation for a QuikSCAT wind speed and an SSM/I wind speed to be compared were 30 km and 167 min, respectively. Note that the cutoff value of 3 m s^{-1} for QuikSCAT wind speeds resulted from the ambiguity removal algorithm (i.e., direction interval retrieval with threshold nudging wind vector solution), which selected the best wind vector among up to four ambiguities. On average, the wind measured by SSM/I was 2.2 m s^{-1} greater than by QuikSCAT.

b. 3DVAR analysis

Figure 6 shows the increments of wind vectors at 950 hPa (i.e., 3DVAR analysis minus first guess). The maximum values were 6.6 , 8.3 , and 6.0 m s^{-1} from SSW, QCAT, and NDQCAT, respectively. For reference, it is worth mentioning again that the satellite swath passing through the storm is 36 (73) min earlier (later) than the model initial time (0000 UTC 19 September 2002) for QuikSCAT (SSM/I) data. While a positive cyclonic circulation increment was obtained after assimilation of SSM/I and QuikSCAT data, it is interesting to note how significant their differences are. The increment pattern from the QuikSCAT analysis is more complicated due to the relocation of the storm, a positive result from the assimilation of wind vectors. A divergence feature of the increment was seen from QCAT (Fig. 6b) but not from SSW (Fig. 6a). Without wind direction information, the assimilation of SSM/I winds mainly enhances the circulation. This is also clearly shown in the NDQCAT analysis, which assimilates only QuikSCAT wind speeds. The pattern of wind increments from NDQCAT was very similar to that from SSW (i.e., Fig. 6c versus 6a), in particular in the vicinity

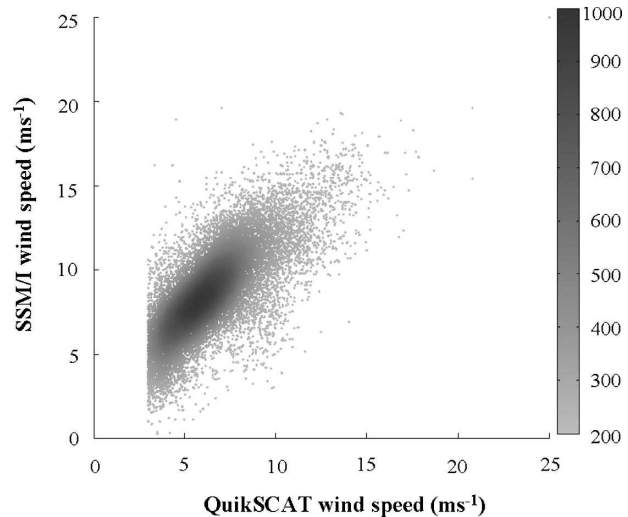


FIG. 5. Point density plot (points/area) of QuikSCAT vs SSM/I wind speeds (21 247 points). Data were collected from 1200 UTC 17 Sep to 1200 UTC 23 Sep 2002 within domain 1 (every 12 h with a 3-h time window). The maximum and minimum time differences between two observations are 167 and 68 min, respectively. Note that the cutoff value of 3 m s^{-1} for QuikSCAT wind speeds is due to the use of the ambiguity removal algorithm (i.e., direction interval retrieval with threshold nudging wind vector solution), which selects the best wind vector among up to four ambiguities.

of the storm from the first guess. The position errors from these two experiments were also very similar (Fig. 7 and Table 3) and showed almost no improvement compared with the CNTL experiment.

The assimilation of QuikSCAT wind vectors (i.e., QCAT) adjusted the initial storm position so that it was closer to the best-track one (Figs. 6b and 7b). Compared with results from NDQCAT, the storm position error was reduced by almost 35% (dots N and O in Fig. 7b and Table 3). Figure 6d shows the difference of wind vectors between ALL and QCAT; the maximum difference was 3.8 m s^{-1} . The cyclonic circulation and the divergence increments to the west and south of the observed, respectively, as well as the change of the storm position (dot A in Fig. 7b) reflect the influence from both satellite winds. All these 3DVAR analyses indicate that the SSM/I data is responsible for the incorrect increment near the CNTL hurricane center location. The best analysis of Hurricane Isidore is obtained when only QuikSCAT wind vectors are assimilated.

The results of TSSW and TQCAT wind increments and storm position errors were very similar to SSW and QCAT, respectively, and are not shown. The patterns of total column water vapor increments from TSSW, TQCAT, and ALL are very similar to the moisture innovation in Fig. 4a (figures are not shown either).

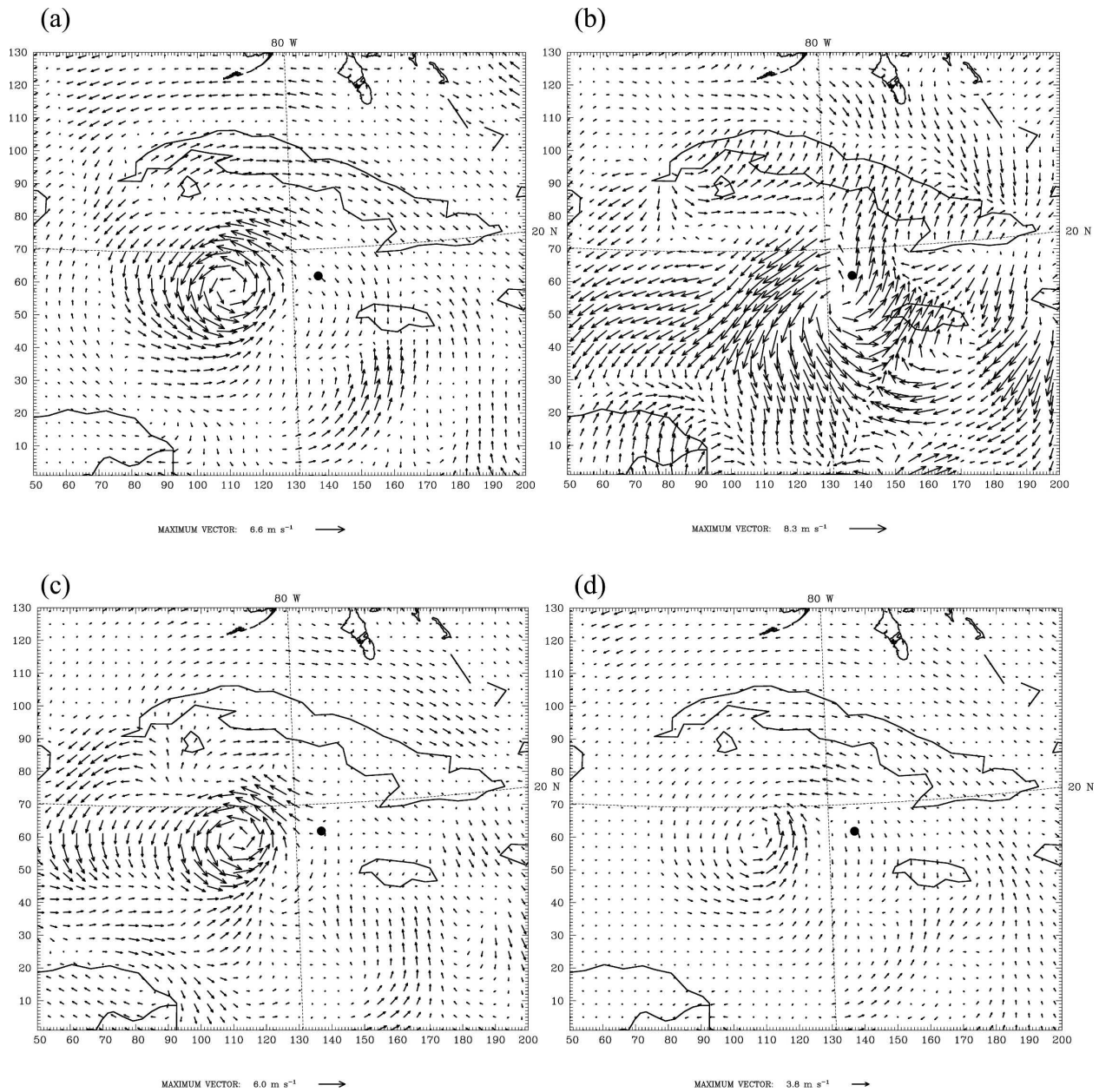


FIG. 6. The differences of the 950-hPa wind vectors between (a) SSW and CNTL experiments, (b) QCAT and CNTL experiments, (c) NDQCAT and CNTL experiments, and (d) ALL and QCAT experiments at 0000 UTC 19 Sep 2002. The black dot indicates the best-track position of the observed storm.

c. Simulation results

1) STORM INTENSITY

Figures 8a,b show the time evolution of the best-track and simulated SLP at the storm's center and the maximum low-level wind speed, respectively. The best-track SLP was 998 hPa at the model initial time (i.e., 0000 UTC 19 September 2002) and dropped to 947 hPa 72 h later. During the first 30 h, the SLP at the storm's

center decreased dramatically while the maximum low-level wind intensified. During the next 24 h, the maximum low-level wind weakened, while the SLP approached an approximately steady state (deepened only 3 hPa within 24 h). This 24-h period closely corresponded to the activity from the time before, during, and after Isidore's landfall in Cuba (Fig. 1). The friction and the reduction of heat flux supply from the surface may well explain this weakening process. Between 54

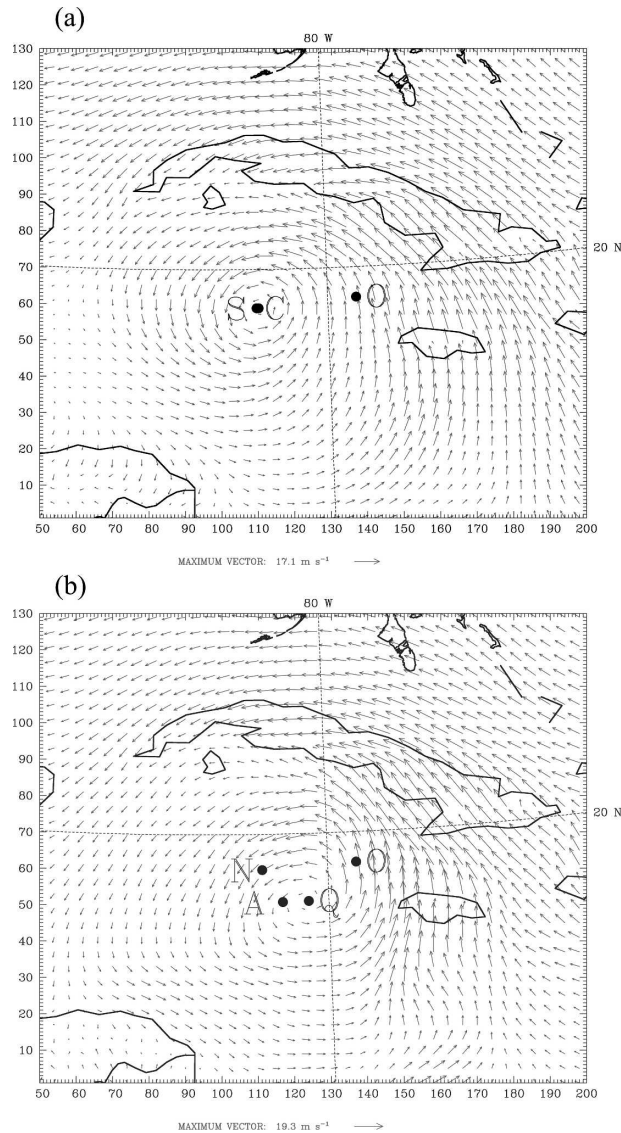


FIG. 7. The 950-hPa wind vectors from (a) SSW and (b) QCAT at 0000 UTC 19 Sep 2002. Dots represent the position of storm center, defined by the 950-hPa wind field, from the best-track position (O) and model simulations. Letters C, S, Q, N, and A denote CNTL, SSW, QCAT, NDQCAT, and ALL experiments, respectively.

and 66 h, back over warm ocean, the best-track storm quickly deepened again and between 66 and 72 h the pressure increased slightly.

The simulated SLP at the storm center from the CNTL experiment was very weak during the first 42-h simulation and intensified for the next 18 h, as shown in Fig. 8. After a 72-h simulation, the SLP dropped to 980 hPa (represented as a thick solid black line), which is about 33 hPa higher than the best-track SLP. The maximum low-level wind speed from CNTL remained weak during the first 18-h simulation and then gradually

TABLE 3. The storm position error (km) at model initial time for CNTL, SSW, QCAT, NDQCAT, and ALL experiments.

Case	Error (km)
CNTL	252.12
SSW	257.3
QCAT	158.1
NDQCAT	243.0
ALL	215.2

strengthened for the next 48 h. At the end of the simulation, the simulated wind speed was 28.3 m s^{-1} weaker than the best track.

Comparing SSM/I and QuikSCAT data, the assimilation of either wind observations (i.e., SSW versus QCAT and TSSW versus TQCAT) significantly improved simulated SLP for the first 30 h, the time when the observed storm was intensifying. Results from different experiments began to diverge after the simulated storm's approach to Cuba. None of the experiments were able to capture the steady-state period (i.e., 30–54 h) as was observed because of the inaccurate timing and location of landfall in the simulations. Simulated minimum SLP from TQCAT, as well as ALL, at least showed the correct strength during the steady-state period, though the period started almost 18 h late. When either satellite data were assimilated (i.e., SSW, TSSW, QCAT, and TQCAT), the errors from these four experiments were small and remained almost constant for the first 2 days (Fig. 9a). However, the errors grew quickly during the last day of simulations, except for the QCAT whose simulated SLP was about 7 hPa higher than the best-track value at the end of the 72-h simulation.

Although the simulated maximum low-level winds from QCAT, TQCAT, SSW, and TSSW slightly overshoot the best-track values at the early stage of the simulation, the simulated trend and magnitudes followed the best-track ones quite well during the first 30-h simulation. The errors were significantly reduced compared with those from CNTL after the assimilation of either satellite winds, in particular for the assimilation of SSM/I (i.e., SSW and TSSW). But as with simulated SLP the errors grew quickly for the last day of the simulation (Fig. 9b). The assimilation of wind vectors was able to reduce the error growth rate for both SLP and maximum low-level wind during the last 24-h simulation (Fig. 9).

From the first 48-h simulated maximum low-level winds, one may think that SSM/I winds have a slightly better impact on the accuracy of Isidore simulations than QuikSCAT winds (Fig. 9b). However, it is important to keep in mind that SSM/I winds tended to be overestimated in this case study. Therefore, the exag-

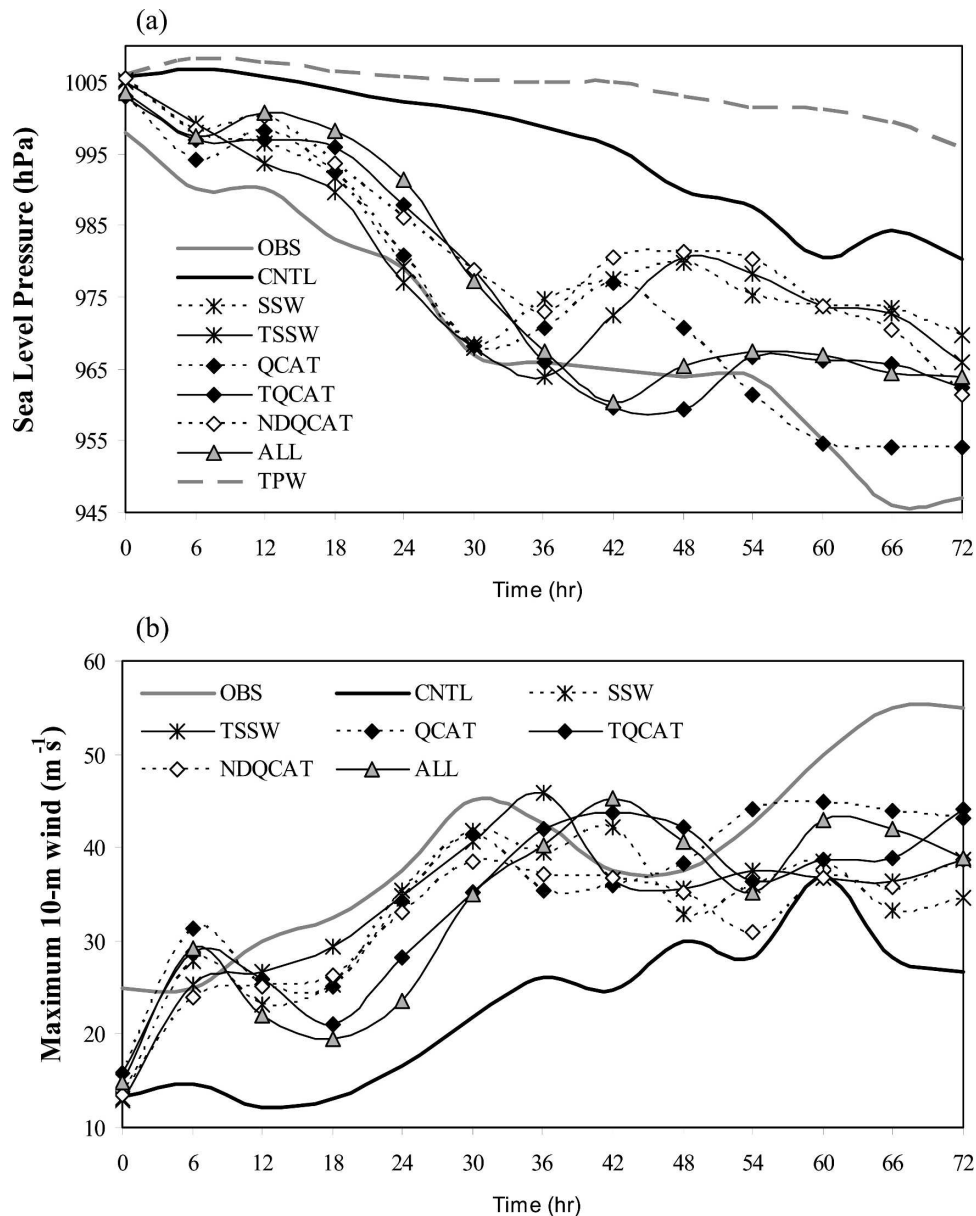


FIG. 8. Time evolution of (a) the minimum SLPs (hPa) at the storm center and (b) the maximum 10-m winds from the best-track information (OBS) and model simulations. TPW assimilated only SSM/I total column water vapor.

gerated impact from the faster SSM/I winds might compensate for the weak winds in the first guess fields (two wrongs make a right).

The simulated storm intensity from NDQCAT, which assimilates only QuikSCAT wind speed, had very similar results as those from SSW (Figs. 8 and 9). The simulated SLP and maximum low-level wind from experiment ALL were comparable overall with those from TQCAT, but slightly worse during the first day's simulation. The error growth rate for the third day was also reduced compared with that from SSW, TSSW, or

NDQCAT due to the assimilation of QuikSCAT wind directions. As mentioned before, the assimilation of SSM/I total column water vapor alone degraded the simulated SLP (thick dashed gray line in Fig. 8a). Compared with QCAT, the addition of assimilating this moisture data in TQCAT had a slightly negative impact on simulated storm intensity, in particularly for the last day.

2) STORM TRACK

The time evolution for the simulated track errors is shown in Fig. 10. The errors from the CNTL experi-

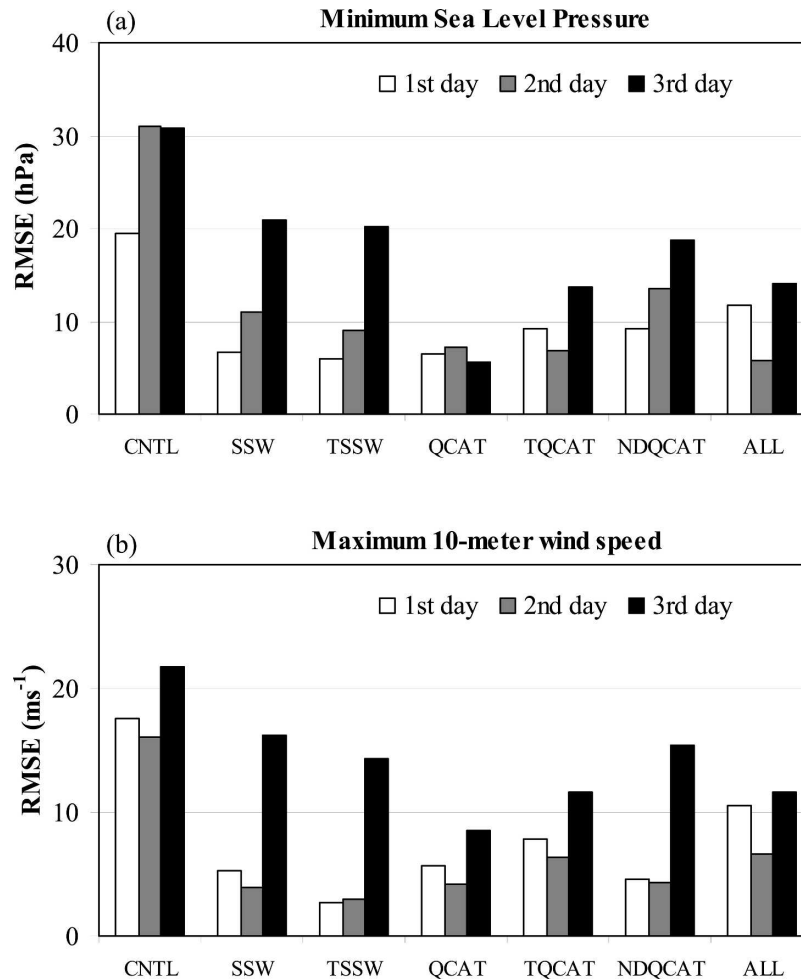


FIG. 9. RMSE of the simulated (a) minimum SLPs (hPa) at the storm center and (b) maximum 10-m wind speed during the first-, second-, and third-day integrations, where error is defined as the difference of the simulated storm center from the best-track position.

ment after 24-, 48-, and 72-h simulations were 196, 208, and 315 km, respectively, which are comparable to the errors from the official averaged forecast (102, 187, and 328 km for the 24-, 48-, and 72-h forecasts, respectively) for the last 2 days but worse for the first day. Compared with CNTL, the assimilation of SSM/I wind speeds with or without SSM/I total column water vapor (i.e., SSW and TSSW in Fig. 10) improved the simulated track only during the 12–42-h simulation period, while the inclusion of QuikSCAT wind vectors (i.e., QCAT, TQCAT, and ALL in Fig. 10) consistently reduced track errors during the entire simulation period. Although the results from NDQCAT, which assimilates QuikSCAT wind speed, are better than those from SSW during the 24–54-h simulation, their conclusions are similar and this confirms our hypothesis for the assimilation of wind directions and is in agreement with Figs. 6a,c.

Figure 11 shows 72-h observed (from the best track) and simulated tracks. As mentioned earlier, the storm position is defined by flow circulation at 950 hPa (i.e., minimum wind speed). The observed hurricane gradually turned in a westerly and then southwesterly direction after 0000 UTC 21 September 2002. Without the assimilation of SSM/I moisture (Fig. 11a), QCAT is the only simulation that produced a nice turn to the west followed by a slight movement toward the southwest as the best-track positions. However, the QCAT-simulated position was about 240-km north of the best-track observation during the last day of simulation. The assimilation of SSM/I moisture and QuikSCAT winds (i.e., TQCAT) resulted in a smaller error compared with QCAT during the last day of simulation, and the simulated storm also turned to the west as the best-track observation. When SSM/I winds and total column

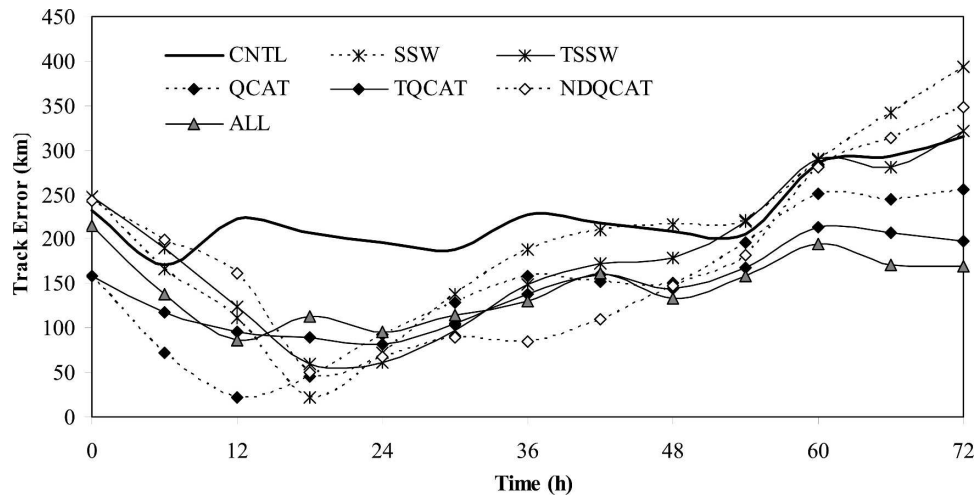


FIG. 10. Time evolution of simulated track error (km), which is defined as the difference of the simulated storm center from the best-track position, for all simulations.

water vapor were assimilated (i.e., TSSW), the third day showed the simulated storm starting to turn toward the west, which is not seen in the SSW experiment (the simulated position was still too far northeast of the best-track one). The results consistently show that the assimilation of SSM/I moisture results in a slightly improved simulated track during the later period of the simulation, when compared to the corresponding no-moisture assimilation experiments (i.e., QCAT versus TQCAT after the 48-h simulation and SSW versus TSSW after the 24-h simulation in Figs. 10 and 11). The improvement of the initial storm position (Fig. 7 and Table 3) partially explains the error reduction for QCAT, TQCAT, and ALL. However, the improvement due to the assimilation of SSM/I moisture may just be a coincidence and further investigation is required to generalize that conclusion.

3) LATENT HEAT FLUX AND RADAR ECHO

Figure 12 shows the latent heat flux 12 h into the simulations. The assimilation of SSM/I and/or QuikSCAT winds strengthened the initial wind field. The stronger low-level winds then increased air–sea interactions (Esbensen et al. 1993; Liu 1988), which resulted in a greater heat flux from the ocean’s surface (i.e., Figs. 12b–f versus 12a). This increase in heat flux is an important physical process in hurricane development. To demonstrate this, an experiment with the same initial and boundary conditions as SSW but without surface latent heat flux was conducted. Results show that the simulated storm does not develop and the simulated SLP after a 72-h simulation is 1015 hPa, which is 45 hPa higher than that from SSW.

Figure 13 shows the observed and simulated radar echoes of the same domain size (360 km \times 360 km) at 0000 UTC 22 September 2002 (i.e., the 72-h simulations). A wider cloud band to the eastern and northeastern sides of the storm is observed (top in Fig. 13), and this band was reproduced by model simulations, excepting the CNTL and TSSW experiments (note that the result from TSSW is still better than from CNTL). The simulated storm structure from CNTL was not well organized (Fig. 13a) and was thus significantly improved upon by assimilation of SSM/I and/or QuikSCAT winds (i.e., QCAT and SSW). The Isidore eye was better simulated after the assimilation of QuikSCAT data than SSM/I data (i.e., QCAT versus SSW and TQCAT versus TSSW). Unfortunately, the addition of assimilating SSM/I moisture degraded the simulated radar echo (i.e., SSW versus TSSW and QCAT versus TQCAT). The simulated radar echo from the experiment ALL was also quite good, in particular, the second cloud band to the northeast of the hurricane eye was better simulated compared with other experiments.

5. Summary

The impact of SSM/I-retrieved products and QuikSCAT winds on the Hurricane Isidore simulation was assessed using the MM5 model and its 3DVAR system. Hurricane Isidore is a good case for this study for the following two reasons. One is the availability of three independent datasets that overlap in the vicinity of the hurricane at the model initial time (i.e., SSM/I, QuikSCAT, and GPS dropsondes). The other is that weak winds and a misplaced circulation in the initial condi-

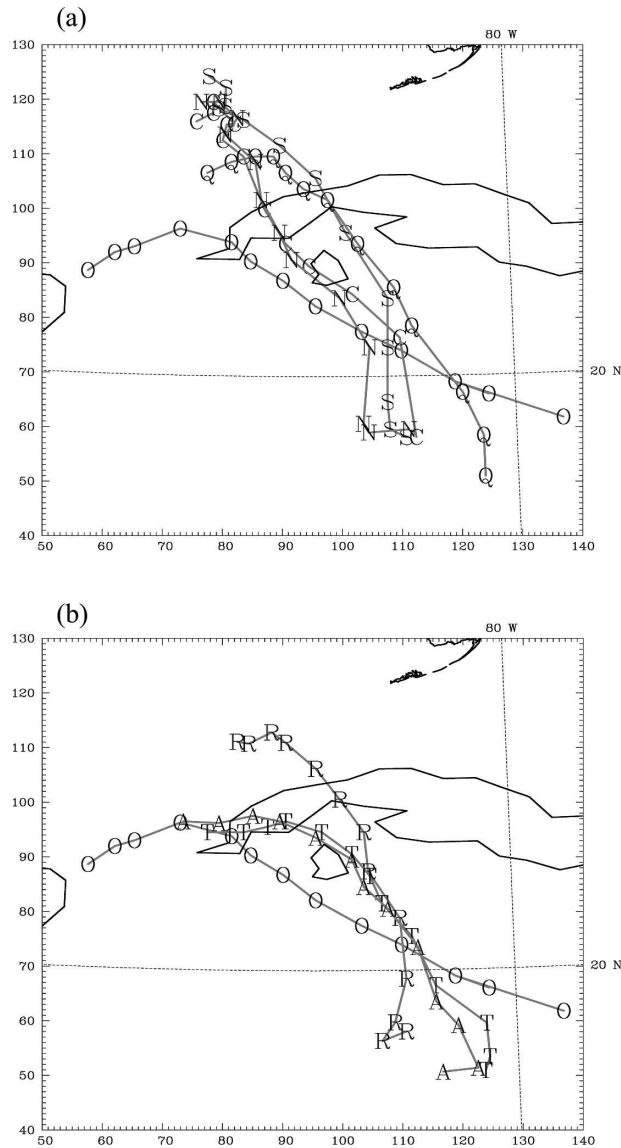


FIG. 11. Tracks of the storm center for the 72-h period ending at 0000 UTC 22 Sep 2002 for (a) the best-track position (O), CNTL (C), SSW (S), QCAT (Q), and NDQCAT (N), and (b) the best-track position (O), TSSW (R), TOCAT (T), and ALL (A) from domain 2.

tions of the CNTL run is very likely a primary reason for the poor numerical simulation and our primary interest is to study satellite-observed winds from SSM/I and QuikSCAT.

Comparisons among three independent datasets were then made. Though only a few soundings are available, SSM/I and QuikSCAT winds were about 1.9 and 0.3 m s^{-1} on average stronger than those from dropsonde data, respectively. From comparisons of more than 20 000 collocated SSM/I and QuikSCAT data, SSM/I wind speed was approximately 2.2 m s^{-1}

stronger than QuikSCAT. Both results allowed us to hypothesize that SSM/I retrieved winds might be overestimated, at least for this particular case study. Comparison with the wind direction from dropsondes shows that the quality of QuikSCAT-retrieved wind directions is very good, with a standard deviation error of about 20° .

The assimilation of SSM/I (i.e., SSW) or QuikSCAT (i.e., QCAT) winds strengthened the cyclonic circulation in the analysis (i.e., initial conditions). As a result, the simulated storm intensity (i.e., the SLP and the maximum low-level wind) was significantly improved. During the first 2 days of the simulations, the SLP and maximum low-level wind errors were reduced by more than half compared with the CNTL experiment and remained almost constant. However, the errors grew quickly during the last day of simulations. The simulated maximum low-level wind speed from SSW was slightly better than that from QCAT during the first 2 days of the simulations. This might be due to the overestimation of SSM/I winds, which may compensate for the underestimated winds in the first guess. The positive increment of low-level winds can enhance the process of air-sea interaction, which is critical to hurricane evolution over the ocean. In addition to the improvement of storm intensity, the storm structure was better simulated.

In addition to a slightly better quality of wind speed, QuikSCAT data are superior to SSM/I-observed winds because they contain wind direction information. The possibility exists that a hurricane, cyclone, or frontal system position over the ocean may be misrepresented at the model initial time. In this case, good quality information on wind direction can potentially correct the initial location of the system, thus affecting the simulated system intensity and track. In this study, the assimilation of QuikSCAT wind vectors (i.e., QCAT) helped correct the simulated storm position toward the best track at the model initial time. This results in a clear improvement of the simulated track over SSW during almost the entire simulation period. The effect of the wind direction is further confirmed by the NDQCAT experiment, which assimilated QuikSCAT wind speed only. In addition, without the assimilation of SSM/I moisture, QCAT is the only simulation that makes a very nice west-southwest turn as the best-track position of the observed storm after a 48-h simulation when the system moves away from Cuba. This track prediction improvement can be partially explained by the improvement on the storm position in model initial conditions.

The analysis after assimilating SSM/I and QuikSCAT

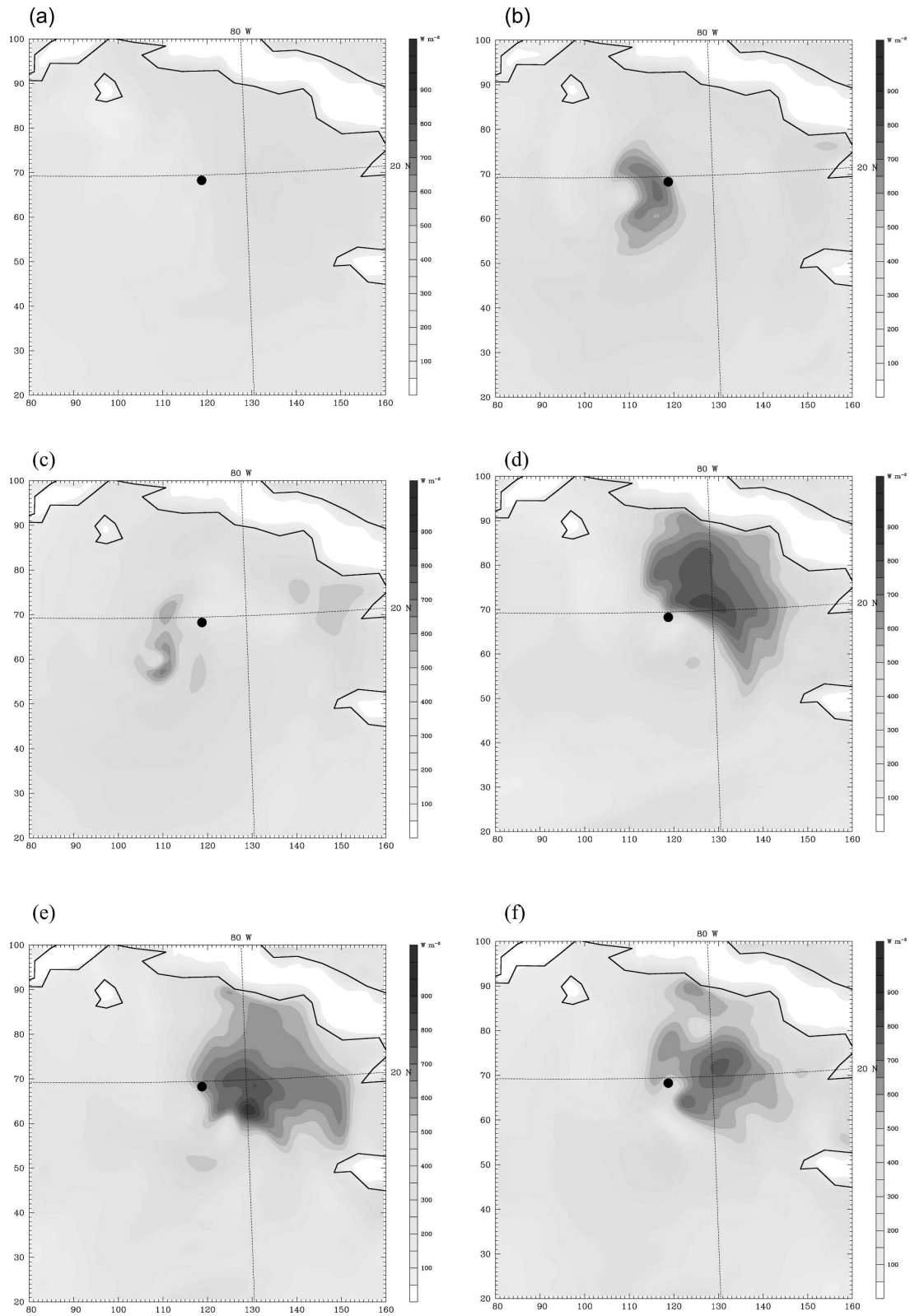


FIG. 12. The latent heat flux (W m^{-2}) 12 h into the (a) CNTL, (b) SSW, (c) TSSW, (d) QCAT, (e) TQCAT, and (f) ALL simulations (i.e., 0000 UTC–1200 UTC 19 Sep 2002). The black dot indicates the best track position of the observed storm at 1200 UTC 19 Sep 2002.

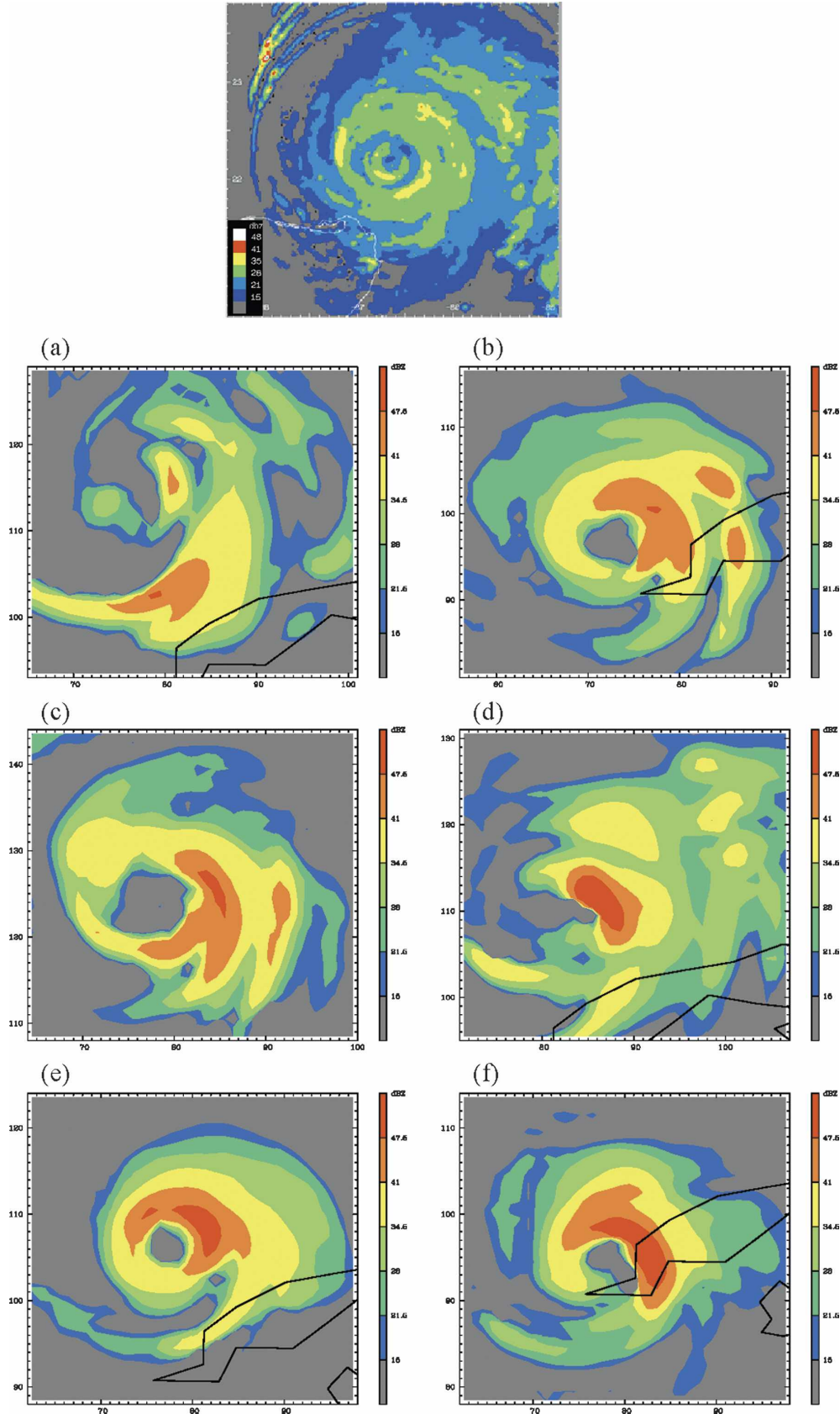


FIG. 13. (top) Observed and (a)–(f) simulated radar echoes (dBZ) valid at 0000 UTC 22 Sep 2002 (72-h simulation) for experiments (a) CNTL, (b) ALL, (c) SSW, (d) TSSW, (e) QCAT, and (f) TQCAT. All plots have the same sized domain, 360 km × 360 km.

(i.e., ALL) is a mixture between TQCAT, which assimilates QuikSCAT winds and SSM/I moisture, and TSSW, which assimilates SSM/I winds and moisture. The simulated intensity from ALL is comparable with that from TQCAT but slightly worse during the first day.

When the wind field in the initial condition is poor, either SSM/I or QuikSCAT winds have a potential to improve model simulations or forecasts. In this particular case study, the assimilation of SSM/I or QuikSCAT data has a greater impact on the first 2 days of simulation when errors are near constant, and the addition of assimilating wind direction can improve the simulated storm track. However, the impact of SSM/I or QuikSCAT winds on Isidore simulations will be less significant if other observations are used in the CNTL experiment, such as dropsondes and other available satellite data. In addition, results presented in this study are based on one case only. It will require more case studies in order to reach a more general conclusion.

Acknowledgments. The authors thank the MM5 3DVAR group for their effort on the development. Further thanks are given to J.-D. Chen at NASA and J. F. Bresch at NCAR for helpful discussions, to A. Chen for preparing QuikSCAT data, to Z. Zhao for plotting Fig. 5, and to M. H. Lin for proofreading the manuscript. Thanks are also extended to Dr. S. M. Leidner and the anonymous reviewers for their extensive and valuable comments that helped to improve the manuscript. The SSM/I data were obtained from the Global Hydrology Resource Center at the Global Hydrology and Climate Center, NASA, Huntsville, Alabama. The QuikSCAT data were provided by the Physical Oceanography Distributed Active Archive Center, Jet Propulsion Laboratory, NASA. GPS dropsonde data were provided at the courtesy of the NOAA/AOML/Hurricane Research Division in Miami, Florida.

REFERENCES

- Atlas, R., and Coauthors, 2001: The effects of marine winds from scatterometer data on weather analysis and forecasting. *Bull. Amer. Meteor. Soc.*, **82**, 1965–1990.
- Barker, D. M., W. Huang, Y.-R. Guo, A. J. Bourgeois, and Q. N. Xiao, 2004: A three-dimensional variational data assimilation system for MM5: Implementation and initial results. *Mon. Wea. Rev.*, **132**, 897–914.
- Bender, M. A., R. J. Ross, R. E. Tuleya, and Y. Kurihara, 1993: Improvements in tropical cyclone track and intensity forecasts using the GFDL initialization system. *Mon. Wea. Rev.*, **121**, 2046–2061.
- Boutin, J., and J. Etcheto, 1996: Consistency of GEOSAT, SSM/I, and *ERS-1* global surface wind speeds—Comparison with in situ data. *J. Atmos. Oceanic Technol.*, **13**, 183–197.
- Chen, S.-H., F. Vandenbergh, G. W. Petty, and J. F. Bresch, 2004: Application of SSM/I satellite data to a hurricane simulation. *Quart. J. Roy. Meteor. Soc.*, **130**, 801–825.
- Courtier, P., J.-N. Thepaut, and A. Hollingsworth, 1994: A strategy for operational implementation of 4D-Var using an incremental approach. *Quart. J. Roy. Meteor. Soc.*, **120**, 1367–1387.
- Esbensen, S. K., D. B. Chelton, D. Vickers, and J. Sun, 1993: An analysis of errors in Special Sensor Microwave Imager evaporation estimated over the global ocean. *J. Geophys. Res.*, **98**, 7081–7101.
- Grell, G. A., J. Dudhia, and D. R. Stauffer, 1994: A description of the fifth-generation Penn State/NCAR mesoscale model (MM5). NCAR/TN-398+STR, National Center for Atmospheric Research, Boulder, CO, 122 pp.
- Halpern, D., 1993: Validation of Special Sensor Microwave Imager monthly-mean wind speed from July 1987 to December 1989. *IEEE Trans. Geosci. Remote Sens.*, **31**, 692–699.
- , A. Hollingsworth, and F. Wentz, 1994: ECMWF and SSM/I global surface winds speeds. *J. Atmos. Oceanic Technol.*, **11**, 779–788.
- Hollinger, J., 1989: DMSP Special Sensor Microwave/Imager calibration/validation. Naval Research Laboratory, Final Rep., Vol. 1, Washington, DC, 153 pp.
- Hong, S.-Y., and H.-L. Pan, 1996: Nonlocal boundary layer vertical diffusion in a medium-range forecast model. *Mon. Wea. Rev.*, **124**, 2322–2339.
- Isaksen, L., and A. Stoffelen, 2000: ERS scatterometer wind data impact on ECMWF's tropical cyclone forecasts. *IEEE Trans. Geosci. Remote Sens.*, **38**, 1885–1892.
- , and P. A. E. M. Janssen, 2004: Impact of ERS scatterometer winds in ECMWF's assimilation system. *Quart. J. Roy. Meteor. Soc.*, **130**, 1793–1814.
- Kain, J. S., 2004: The Kain–Fritsch convective parameterization: An update. *J. Appl. Meteor.*, **43**, 170–181.
- Kalnay, E., and Coauthors, 1996: The NCEP/NCAR 40-Year Reanalysis Project. *Bull. Amer. Meteor. Soc.*, **77**, 437–471.
- Krasnopolsky, V., L. Breaker, and W. Gemmill, 1995: A neural network as a nonlinear transfer function model for retrieving surface winds speeds from the Special Sensor Microwave Imager. *J. Geophys. Res.*, **100**, 11 033–11 045.
- Kurihara, Y., M. Bender, and R. J. Ross, 1993: An initialization scheme of hurricane models by vortex specification. *Mon. Wea. Rev.*, **121**, 2030–2045.
- Leidner, S. M., L. Isaksen, and R. N. Hoffman, 2003: Impact of NSCAT winds on tropical cyclones in the ECMWF 4DVAR assimilation system. *Mon. Wea. Rev.*, **131**, 3–26.
- Li, Z., I. Navon, and Y. Zhu, 2000: Performance of 4DVAR with different strategies for the use of adjoint physics with the FSU global spectral model. *Mon. Wea. Rev.*, **128**, 668–688.
- Liu, W. T., 1988: Moisture and latent heat flux variability in the tropical Pacific derived from satellite data. *J. Geophys. Res.*, **93**, 6749–6760.
- Lorenc, A. C., and Coauthors, 2000: The Met. Office global three-dimensional variational data assimilation scheme. *Quart. J. Roy. Meteor. Soc.*, **126**, 2991–3012.
- Mears, C. A., D. K. Smith, and F. J. Wentz, 2001: Comparison of Special Sensor Microwave Imager and buoy-measured wind speeds from 1987 to 1997. *J. Geophys. Res.*, **106**, 11 719–11 729.
- Meissner, T., D. Smith, and F. Wentz, 2001: A 10 year intercomparison between collocated Special Sensor Microwave Imager oceanic surface wind speed retrievals and global analyses. *J. Geophys. Res.*, **106**, 11 731–11 742.

- Parrish, D. F., and J. C. Derber, 1992: The National Meteorological Center's spectral statistical-interpolation analysis system. *Mon. Wea. Rev.*, **120**, 1747–1763.
- Phalippou, L., 1996: Variational retrieval of humidity profile, wind speed and cloud liquid water path with the SSM/I: Potential for numerical weather prediction. *Quart. J. Roy. Meteor. Soc.*, **122**, 327–355.
- Rabier, F., H. Jaervinen, E. Klinker, J.-F. Mahfouf, and A. Simmons, 2000: The ECMWF operational implementation of four-dimensional variational assimilation. Part I: Experimental results with simplified physics. *Quart. J. Roy. Meteor. Soc.*, **126**, 1143–1170.
- Rienecker, M. M., R. Atlas, S. D. Schubert, and C. S. Willett, 1996: A comparison of surface wind products over the North Pacific Ocean. *J. Geophys. Res.*, **101**, 1011–1023.
- Shaffer, S. J., R. S. Dunbar, S. V. Hsiao, and D. G. Long, 1991: A median-filter-based ambiguity removal algorithm for NSCAT. *IEEE Trans. Geosci. Remote Sens.*, **29**, 167–174.
- Stogryn, A., C. Butler, and T. Bartolac, 1994: Ocean surface wind retrievals from special sensor microwave imager data with neural networks. *J. Geophys. Res.*, **99**, 981–984.
- Waliser, D. E., and C. Gautier, 1993: Comparison of buoy and SSM/I-derived wind speeds in the tropical Pacific. *TOGA Notes*, No. 12, 1–7.
- Wentz, F. J., 1993: User's manual SSM/I antenna temperature tapes revision 2. RSS Tech. Rep. 120193, Remote Sensing Systems, Santa Rosa, CA, 13 pp.
- , and D. K. Smith, 1999: A model function for the ocean normalized radar cross section at 14 GHz derived from NSCAT observations. *J. Geophys. Res.*, **104**, 11 499–11 514.
- Yu, T.-W., M. Iredell, and D. Keyser, 1997: Global data assimilation and forecast experiments using SSM/I wind speed data derived from a neural network algorithm. *Wea. Forecasting*, **12**, 859–865.
- Yuan, X., 2004: High-wind-speed evaluation in the Southern Ocean. *J. Geophys. Res.*, **109**, D13101, doi:10.1029/2003JD004179.
- Zou, X., and Q. Xiao, 2000: Studies on the initialization and simulation of a mature hurricane using a variational bogus data assimilation scheme. *J. Atmos. Sci.*, **57**, 836–860.